

CCTA-PET Registration for Quantitative Analysis of Myocardial Infarction

Zhenzhen Xu¹, Bo Tao², Heng Zhao¹, Feng Cao², Jimin Liang*

¹Engineering Research Center of Molecular and Neuro Imaging of Ministry of Education School of Life Science and Technology, Xidian University Xi'an, Shaanxi 710071, China

²Department of Cardiology Chinese PLA General Hospital Beijing 100853, China

Abstract—Quantitative analysis of myocardial infarction is important for the prognostic assessment and therapeutic strategy of patients with ischemic heart disease (IHD). ¹⁸F-fluorodeoxyglucose (FDG) PET is generally regarded as the gold standard for *in vivo* assessing myocardial viability. However, currently PET scans can only be interpreted by well trained radiologists because the morphological variation and location of infarct myocardium is hard to reflect visually on 2D slices or polar plot. In this paper, a 3D non-rigid coronary CTA (CCTA)-PET registration strategy is presented to quantitative analysis the extent of myocardial infarction. Whole heart is firstly segmented from both CCTA and PET/CT. Then the myocardium of left ventricle (LV) is separated from CCTA and PET/CT, respectively. After morphological post-processing, the myocardium image is integrated with the whole heart image both for CCTA and PET/CT to conduct the myocardial registration. A random forest classifier is trained to identify the infarct area of LV wall. The myocardial infarction analysis method proposed in this paper is compared with the cardiac tissue histological study. The result demonstrates good agreement with the TTC stain result in both infarct size and location, and suggests a potential value for clinic application in the prognosis of myocardial infarction.

Keywords—Coronary CTA; PET; multimodality registration; quantitative analysis; myocardial infarction

I. INTRODUCTION

¹⁸F-fluorodeoxyglucose (FDG) positron emission tomography (PET) is generally regarded as the gold standard for myocardial viability assessment [1-3]. So far radiologists typically view PET data in 2D slices or based on the polar plot[4] (“bull’s-eye”) images in which the entire heart is displayed in a 2D circular representation with the apex in the middle, and the periphery representing the anterior, lateral, inferior, and septal walls. However, the interpretation of either the 2D slices or the bull’s-eye images requires a great deal of experience and dedicated studies. In order to assist radiologists in monitoring the myocardial viability of patients in an intuitive way, some studies adopted the coronary computed tomography angiography (CCTA)-PET fusion methods [5-7] in that the combination of multimodality images was demonstrated to provide comprehensive information. However, the methods in [5-7] all need manual registration. Such a strategy is limited by heavy workload and poor repeatability.

In this paper a quantitative infarct size analysis technique based on automatic CCTA-PET image fusion is presented. The fusion result is displayed in 3D visual form integrating both anatomic information and functional information, distinctly revealing the size and position of infarction. At the same time, we also provide the percentage of infarct area out of the total left ventricular (LV) as a quantitative index. Methods

A. Data acquisition

We built myocardial infarction models in 30 guangxi bama minipigs (male, aged months, 25-30 kg). Balloon occlusion of the left anterior descending (LAD) artery took about 60 min, followed by reperfusion. From three days to three months after the induction of myocardial infarction, animals were placed in a right lateral recumbent position and underwent full-body CCTA scan (SOMATOM Definition dual-source CT, Siemens Medical Systems) and FDG PET/CT scan on a Siemens Biograph 40 PET/CT scanner whose PET system consist of a multi-LSO-detector ring system with 3D acquisition and reconstruction. The details of the model creation can be found in reference [8].

Reconstruction of the raw CCTA data resulted in a volume dataset with a batch of approximately 500 sections, 0.37-mm thickness in a 512×512 matrix. The CT image was composed of approximately 109 sections of 512×512 pixels; the detective element size was $0.98 \times 0.98 \text{ mm}^2$; the section thickness was 2.00 mm. The PET data was composed of 111 sections of 168×168 pixels; the detective element size was $2.03 \times 2.03 \text{ mm}^2$; the section thickness was 2.00 mm.

All operations during animal experiments were in accordance with the National Institutes of Health Guide for the Care and Use of Laboratory Animals. All experiments were performed in accordance with the 1964 Helsinki Declaration. The experimental protocol was reviewed and approved by the Committee on Animal Care, Fourth Military Medical University, China.

B. CCTA-PET Registration

The image registration flow chart is shown in Figure 1 and consists of the following steps.

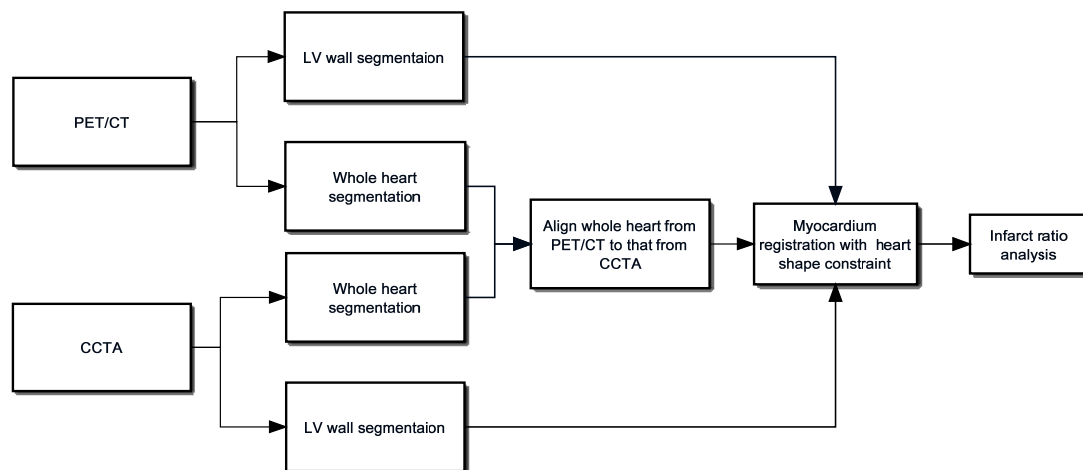


Fig.1. Flow chart of CCTA-PET image fusion

Whole Heart Segmentation: The whole heart regions in CCTA and CT were extracted respectively based on a multi-atlas segmentation method[9]. In this study, 10 atlases for each modality were constructed under the supervision of radiologist by manually labeling the heart region. Majority voting is applied to locally best match the target image, such that the information from poor matching atlases is discarded. The segmentation procedure generates the binary images of heart in CCTA (denoted as $CCTA_h$) and CT (denoted as CT_h) respectively.

Whole Heart Registration: The heart from the CCTA image ($CCTA_h$) is aligned with the heart from the CT (CT_h) via the affine transformation followed by B-spline registration[10]. The generated deformation field is then applied to the functional image PET. The deformed PET image is notes as PET_h . After whole heart alignment, there is still local mismatch between the position of FDG signals and the LV myocardium. Such a mismatch will influence the accuracy of quantitative analysis to some degree. Therefore in this paper, myocardial region alignment is conducted to further improve the registration accuracy. The direct approach is to extract the LV walls from CCTA and PET respectively and align the LV wall from PET to that from CCTA. However, for heart with myocardial infarction, severe perfusion defects may present on PET images that are not visualized in the myocardium on the CCTA scan. Directly applying registration will cause great distortion of the FDG region. So a more reasonable approach is to firstly remove the infarct area in CCTA image and then match the LV wall from PET to that from CCTA.

LV Wall Segmentation: For PET image, a thresholding method is applied to achieve fast myocardium segmentation. According to references[12, 13], a threshold value in the range of $50 \pm 60\%$ of the max value should allow the visualization of viable myocardium. In this paper, 50% of the max pixel value is adopted for myocardium segmentation in PET image. The LV wall from PET is denoted as PET_{LV} . The binary heart from CT (CT_h) is then merged with the LV myocardium PET_{LV} and the result is denoted as PET_f . Consider that severe perfusion defects may present on PET images that are not visualized in

the myocardium on the CCTA scan, applying registration directly will lead to a FDG region distortion. So a more reasonable approach is first remove the infarct area in CCTA image and then match LV wall from PET to that from CCTA.

In CCTA image, LV wall is segmented by region growing (RSG)[11] with the seed points manually selected. The result is denoted as $CCTA_{LV}$. Since the nonviable myocardium tends to be thin after the infarction, a morphological open operation is applied on $CCTA_{LV}$ to remove small pictorials including

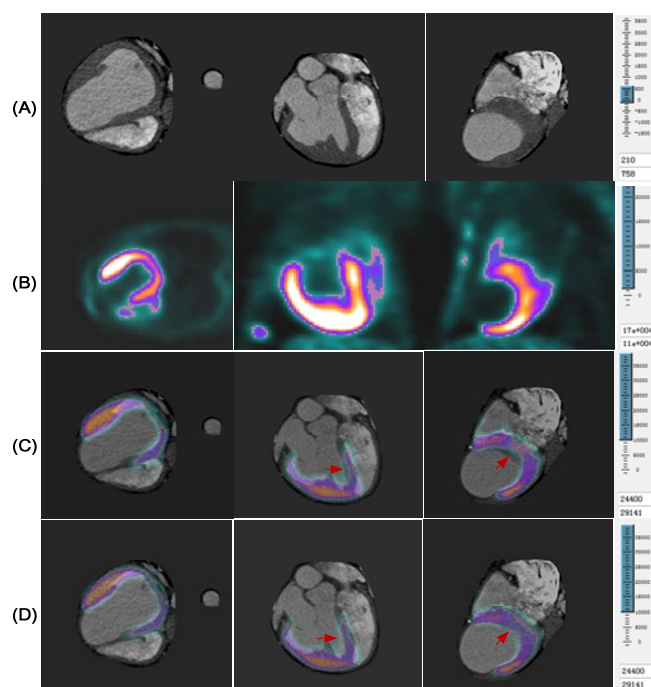


Fig.2. Automated volume alignment of CCTA and PET/CT. Rows from top to bottom show in multiplanar orientations. (A) original CCTA images. (B) Original PET images. (C) PET and CCTA images after whole heart registration. (D) Same images after automatic myocardial registration

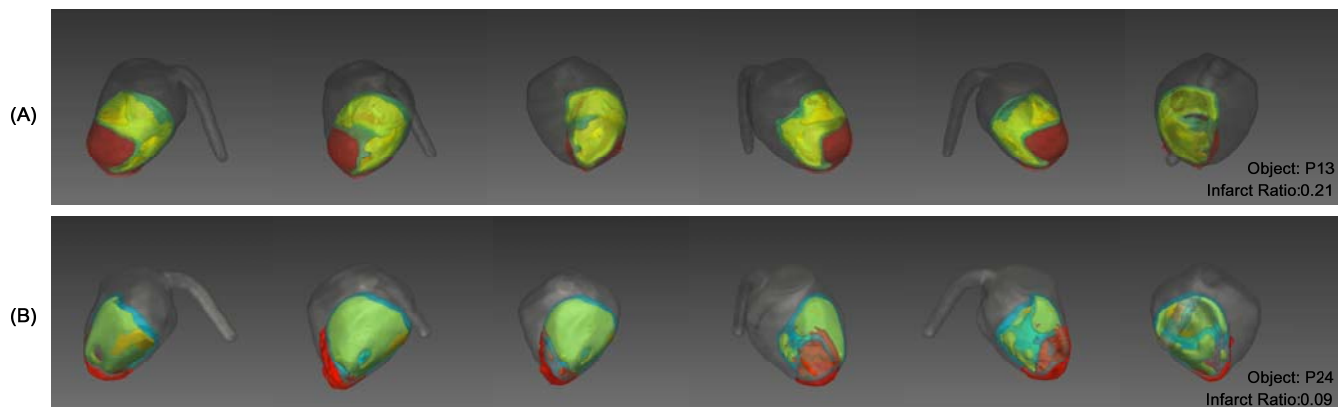


Fig.3. 3D visualization of CCTA-PET fusion. (A) Series of 2D images acquired of P13 of 3D heart structure at different viewing angles. (B) Series of 2D images acquired of P24 of 3D heart structure at different viewing angles.

noise points and thin myocardium regions. The resultant image is denoted as $CCTA'_{LV}$. It's important to note that morphology processing can only roughly remove the nonviable myocardium and assist the following myocardium registration procedure. It cannot be used for accurate calculation of the infarct size.

Myocardium Registration: The whole heart from CCTA ($CCTA_h$) and LV myocardium ($CCTA'_{LV}$) are merged together, denoted as $CCTA_f$, and used as the input of myocardial alignment to guarantee the entirety morphology of heart.

Myocardial alignment of LV wall from CCTA and LV wall from PET/CT is achieved by B-spline registration. The B-spline grid was defined by control points with 20 mm separation. The algorithm optimizes the mutual information (MI) localized similarity measure. We choose the conjugate gradient method as the optimization algorithm. The deformation produced in PET_f to $CCTA_f$ alignment is also applied on PET_h . The result of myocardial alignment is denoted as PET'_h and is shown in Figure 2. From Figure 2 it can be seen, the dislocation of PET signal (pointed out by the red arrow) has been correct effectively after myocardial registration.

Infarct size Analysis: The percentage of infarct area/total LV area is consider to be an index of myocardial injury [14]. However, the infarct size cannot be accurately estimate based on CCTA or PET/CT alone. In this paper, we propose a machine learning method to detect the infarct area in the fusion image of CCTA and PET/CT. A random forest classifier[15] is trained on 5000 image patches with the size of 3×3 pixels. The feature of an image patch is defined as

$$f = [f_p, f_{CCTA}, f_{PET}] \quad (1)$$

where f_p is the 3D position of the center pixel of the image patch, f_{CCTA} and f_{PET} are the vectorized pixel values of the corresponding CCTA and PET images.

The training data set was manually selected and labeled. The parameters of random forest are specified as: number of trees is 100; maximum depth of the tree is 10; feature dimension of each trees is the square-root of total feature

dimension. The five-fold cross-validation is conducted on the training data set and the average accuracy is 86.2%.

Denote the infarct area as $CCTA_{in}$, the ratio of infarct myocardium can be calculated as

$$R_{in} = \frac{|CCTA_{in}|}{|CCTA_{LV}|}, \quad (2)$$

where $|\cdot|$ denotes the number of voxels in image. The quantitative result of 3D CCTA-PET fusion is compared with the triphenyl tetrazolium chloride (TTC) stain to demonstrate the validity of proposed strategy as presented in next section.

After the infarct area has been distinguished using above method, PET'_h is further segmented by thresholding to determine the normal myocardial area. The threshold value $T = 70\% \times \max(PET'_h)$ as suggested in [12, 13]. Finally the rest of myocardium is regarded as dysfunctional myocardium. The three level of FDG uptake is visualized in Figure 3.

II. RESULTS AND ANALYSIS

A. 3D Visualization

Figure 3 shows two examples (minipig P13 and P24) of 3D visualization of CCTA-PET fusion and the quantitative analysis results. The infarct area appears in red. The ischemia area appears in blue and normal in yellow. The normal area is wrapped in ischemia cardiac tissue. Different extent of the glucose metabolism defect as a consequence of the left anterior descending artery infarction can be reflected intuitively on the 3D visualization. For P13, the defect appears in the anterior and apical wall segments of the left ventricle. For P24, the defect only appears in the anterior wall segments of the left ventricle. The infarct size and position coincide well with the TTC stain results shown in Figure 4. From Figure 3, it can also be discovered that the ventricular of P13 had remodeled and cardiac chamber of P13 is dilated. All these phenomenon are most probably caused by ischemia after myocardial infarction[16]. We believe that the 3D CCTA-PET fusion can provide great help for radiologist in determining the heart condition after myocardial infarction.

B. Infarct size

We compare the ratio of infarct area to whole LV wall based on CCTA-PET fusion with the manual calculating result based on TTC stain image. Although the myocardial infarction models were built in 30 minipigs, only 7 objects experimented with TTC pathology analysis. Among which two minipigs contracted pneumonia, resulted in poor uptake of FDG and thus their data are discarded. We conduct the comparison on the remaining 5 minipigs. MI lesion is measured using ImageJ software by manually outline (yellow curve) the infarct area, as shown in Figure 4. The normal tissues are in pink or red color. The infarct tissues are in white.



Fig.4. TTC stain image of (a) P13 and (b) P24

The comparison results are given in Table 1, which shows a good agreement between the 3D quantitative index and that of TTC. The minimum difference is 0.39% and the max difference is 4.87%. The largest difference comes from P34, and the reason is that the pixel value of myocardium in CCTA of P34 is similarity with that of right ventricle. The myocardium is hard to distinguish. It suggests that the myocardium segmentation has an impact on the final result. The consistency between the 3D quantitative result and that of TTC stain demonstrates the feasibility and accuracy of the proposed quantitative analysis strategy.

TABLE I. RATIO OF THE INFARCT AREA

Object number	Ratio(%)		Error
	TTC stain	3D fusion	
P13	21.36%	21.95%	0.59%
P14	14.98%	13.33%	1.65%
P24	7.96%	7.23%	0.73%
P34	18.98%	14.11%	4.87%
P36	9.24%	9.63%	0.39%

III. CONCLUSION

In this paper, a 3D quantitative analysis strategy of myocardial infarction is proposed. Two medical image modality, CCTA and PET/CT, are employed to provide both anatomic and functional information. The multimodality registration is implemented for whole heart and myocardium automatically. The fusion result is presented in 3D visualization with the quantitative index of infarct ratio. Both the infarct size and position is consistent with TTC stain result. To our best knowledge, this is the first study that automatically classifies the LV myocardium after infarction

into three types based on learning method and visualizes the three type's myocardium in 3D. The proposed strategy is efficient and particularly with better interpretability compared with current analysis method, laying foundations for further clinical research and application.

Acknowledgment

This work was supported by the Program of the National Research and Development Program of China under Grant No. 2016YFC1300302, National Natural Science Foundation of China under Grant Nos. 81227901 and 81530058, the Natural Science Basic Research Plan in Shaanxi Province of China under Grant No. 2015JZ019, and the Fundamental Research Funds for the Central Universities (NSIZ021402).

References

- [1] M. M. Al and Z. H. Sun, "Diagnostic value of 18F-FDG PET in the assessment of myocardial viability in coronary artery disease: A comparative study with 99mTc SPECT and echocardiography," vol. 11, pp. 229-236, 2014.
- [2] M. Kobylecka, J. Mączewska, K. Fronczewska-Wieniawska, T. Mazurek, M. T. Płazińska, and L. Królicki, "Myocardial viability assessment in 18FDG PET/CT study (18FDG PET myocardial viability assessment)," *Nuclear Medicine Review Central & Eastern Europe*, vol. 15, pp. 52-60, 2012.
- [3] J. R. McCrary, L. S. Wann, and R. C. Thompson, "PET imaging with FDG to guide revascularization in patients with systolic heart failure," *Egyptian Heart Journal*, vol. 65, pp. 123-129, 2013.
- [4] M. Sciumbata, S. Critello, and D. Galea, "[Quantitative analysis of myocardial glucose metabolism by using dynamic FDG-PET acquisition]," *Recenti Progressi in Medicina*, vol. 103, pp. 450-454, 2012.
- [5] M. Hacker, "Cardiac PET-CT and CT Angiography," *Current Cardiovascular Imaging Reports*, vol. 6, pp. 191-196, 2013.
- [6] W. Tanis, A. Scholtens, J. Habets, V. D. B. Rb, L. A. van Herwerden, S. A. Chamuleau, *et al.*, "CT angiography and ¹⁸F-FDG-PET fusion imaging for prosthetic heart valve endocarditis," *Jacc Cardiovascular Imaging*, vol. 6, pp. 1008-1013, 2013.
- [7] R. Nakazato, D. Dey, E. Alexanderson, A. Meave, M. Jiménez, E. Romero, *et al.*, "Automatic alignment of myocardial perfusion PET and 64-slice coronary CT angiography on hybrid PET/CT," *Journal of Nuclear Cardiology*, vol. 19, pp. 482-491, 2012.
- [8] B. Tao, H. Gao, M. Zheng, Z. Luo, L. Liu, W. Bai, *et al.*, "Preclinical modeling and multimodality imaging of chronic myocardial infarction in minipigs induced by novel interventional embolization technique," *Ejmmi Research*, vol. 6, pp. 1-10, 2016.
- [9] H. A. Kirisli, S. Klein, T. V. Walsum, and W. J. Niessen, "Fully automatic cardiac segmentation from 3D CTA data: a multi-atlas based approach," in *SPIE Medical Imaging*, 2010.
- [10] B. B. Avants, N. J. Tustison, M. Stauffer, G. Song, B. Wu, and J. C. Gee, "The Insight ToolKit image registration framework," *Frontiers in Neuroinformatics*, vol. 8, p. 44, 2014.
- [11] X. H. Wang, B. Liu, and Z. Q. Song, "3-Dimensional Brain MRI Segmentation Based on Multi-Layer Background Subtraction and Seed Region Growing Algorithm," *Applied Mechanics & Materials*, vol. 536-537, pp. 218-221, 2014.
- [12] S. Gargiulo, A. Greco, M. Gramanzini, M. P. Petretta, A. Ferro, M. Larobina, *et al.*, "PET/CT imaging in mouse models of myocardial ischemia," *Journal of Biomedicine & Biotechnology*, vol. 2012, p.: 541872., 2012.
- [13] J. Fleming and J. Fleming, *Quantitative analysis in nuclear medicine imaging*: Springer, 2006.
- [14] J. Lønborg, N. Vejlstrop, H. Kelbæk, L. Nepperchristensen, E. Jørgensen, S. Helqvist, *et al.*, "Impact of acute hyperglycemia on myocardial infarct size, area at risk, and salvage in patients with STEMI and the association with exenatide treatment: results from a randomized study," *Diabetes*, vol. 63, pp. 2474-85, 2014.

- [15] D. F. Polan, S. L. Brady, and R. A. Kaufman, "Tissue segmentation of computed tomography images using a Random Forest algorithm: a feasibility study," *Physics in Medicine & Biology*, vol. 61, pp. 6553-6569, 2016.
- [16] A. Galli and F. Lombardi, "Postinfarct Left Ventricular Remodelling: A Prevailing Cause of Heart Failure," *Cardiology Research & Practice*, vol. 2016, pp. 1-12, 2016.